Scanning Microscopy

Volume 1992
Number 6 *Signal and Image Processing in Microscopy and Microanalysis*

Article 15

1992

Application of the Wavelet Transform to the Digital Image Processing of Electron Micrographs and of Backreflection Electron Diffraction Patterns

A. Gómez
Instituto de Física, U.N.A.M., Mexico

L. Beltrán del Río
Instituto de Física, U.N.A.M., Mexico

D. Romeu
Instituto de Física, U.N.A.M., Mexico

M. Jose Yacamán
Instituto de Física, U.N.A.M., Mexico

Scanning Microscopy Supplement 6, 1992 (pages 153-161) 0892-953X/92$5.00+.00
Scanning Microscopy International, Chicago (AMF O'Hare), IL 60666 USA

APPLICATION OF THE WAVELET TRANSFORM TO THE DIGITAL IMAGE PROCESSING OF ELECTRON MICROGRAPHS AND OF BACKREFLECTION ELECTRON DIFFRACTION PATTERNS

A. Gómez*, L. Beltrán del Río, D. Romeu and M. Jose Yacamán

Instituto de Física, U.N.A.M.
Apartado Postal 20-364, México D.F. C.P. 01000, Mexico

Abstract

In this work we explore the use of the so-called wavelet transform in the digital image processing of micrographs. The wavelet transform of an image f(x,y) is defined as:

$$Wf(s,u,v) = \int_{-\infty}^{\infty}\int_{-\infty}^{\infty} f(x,y)\ s\ \overset{*}{\psi}(s(x-u),s(y-v))\ dxdy$$

where ψ is an analyzing function called "wavelet" and which is in our examples always taken to be the "Mexican hat" given by

$$\psi(x)=(2-(x^2+y^2))\exp(-(x^2+y^2)/2)$$

Some synthetic images are shown in which it can be clearly seen how the wavelet transform can be useful to reveal edges and to emphasize the boundaries of the clusters.

The technique is applied in the case of the CoMoS catalysts, in which the wavelet transform can be used to emphasize the hexagonal domains while filtering the noise quite effectively.The technique is next applied to electron backreflection patterns where substantial noise reduction and emphasis of the lines are achieved.

Several examples of the application of this processing tool to high resolution images of metallic particles and to quasicrystals are presented.

Key Words: Digital image processing, digital filters, electron diffraction, electron microscopy, quasicrystals.

*Address for correspondence:
Alfredo Gómez
Instituto de Física, U.N.A.M.
Apartado Postal 20-364,
México D.F. C.P. 01000, Mexico
Telephone No.: 525-622 5084
Fax No.: 525-616 1535

Introduction

Many of the modern techniques for structural research in materials science provide the information in the form of images. Some examples of this are the transmission electron microscope (in either bright field, dark field or diffraction modes), the scanning electron microscope, the optical microscope and the field ion microscope.

Furthermore, other techniques provide their information in the form of unidimensional signals, the x-ray diffractometer being a good example.

In all these cases, the relevant information can be "masked". For instance, the noise level can be such that it hampers the detection of the information known (or suspected) to be present . Sometimes it is not the noise but the other components of the signal that masks the desired information.

For this reason , over the years many techniques have been developed for the digital processing of images so that noise can be filtered out and the relevant details in the images can be enhanced (Kirkland, 1984; Tomita et al., 1985; De Jong et al., 1989)

Among the digital processing techniques, perhaps those based on the Fourier transform are the most important. With these techniques, the images are analyzed in the frequency domain (i.e. in terms of the periodicities present in the image) rather than in the space domain.

However recently new techniques have been developed that allow a mixed approach, characterizing the images simultaneously in both space and frequency domains (at least to the extent that the "uncertainty principle" permits).

Examples of such techniques are the Wigner distribution, the window Fourier transform (Gabor's transform, or short time Fourier transform) and the wavelet transform.

The purpose of the present work is to explore the use of the wavelet

transform to the digital image processing of transmission electron micrographs and of electron diffraction patterns.

The Wavelet Transform

In the next paragraphs a general overview of wavelet transforms is presented . In order to keep theory simple the one-dimensional case is presented. In the images (which are 2-dimensional) the obvious generalization (section on the Bidimensional Case) is used. Grossman et al. (1985); Mallat, (1989); and Daubechies, (1990) present the theory in much greater detail.

Basic Definitions

Let $\psi(x)$ be a complex-valued function of a real variable (hereafter referred to as wavelet). ψ will be assumed to satisfy the so-called admissibility condition (see section on the admissibility condition below).

Given $s \neq 0$ and u, real numbers, we form the scaled and displaced functions $\sqrt{s}\ \psi(s(x-u))$.

When u=0 we use the shorthand $\psi_s(x)=\sqrt{s}\ \psi(sx)$.

Let f(x) be another complex valued function (the function or "signal" to be analyzed). We define the wavelet transform of f(x) with respect to the wavelet $\psi(x)$ as

$$Wf(s,u)=\int_{-\infty}^{\infty} f(x)\sqrt{s}\ \psi^*(s(x-u))\,dx$$

$$=\int_{-\infty}^{\infty} f(x)\ \psi_s^*(x-u)\,dx \qquad (1)$$

Admissibility condition

It can be shown that, in order to have an inverse for the transform, the wavelet ψ must satisfy the so-called admissibility condition

$$\int_{-\infty}^{\infty}\frac{|\hat{\psi}(\omega)|^2}{|\omega|}d\omega < \infty \qquad (2)$$

where $\hat{\psi}$ denotes the Fourier transform of ψ.

If $\hat{\psi}(\omega)$ decays sufficiently fast as $|\omega| \longrightarrow \infty$ then the admissibility condition amounts to saying that $\hat{\psi}(0)=0$ which in turn implies that, if $\psi(x)$ decays sufficiently fast as $|x| \longrightarrow \infty$

$$\int_{-\infty}^{\infty}\psi(x)\,dx = 0 \qquad (3)$$

The wavelet transform as an inner product

The transform Wf can be written as

$$Wf(s,u)=\langle\psi_s(x-u), f(x)\rangle \qquad (4)$$

where $\langle\ \rangle$ denotes the standard inner product

$$\langle h,f\rangle=\int_{-\infty}^{\infty} h^*(x)\ f(x)\,dx \qquad (5)$$

The wavelet transform as a convolution

Defining $\bar{\psi}_s(x)=\psi_s(-x)$, then

$$Wf(s,u)=[f*\ \bar{\psi}_s^*\ ](u) \qquad (6)$$

where * denotes the operation of convolution defined in general as

$$[h*f](u)=\int_{-\infty}^{\infty} f(x)\ h(u-x)\,dx \qquad (7)$$

Fourier Representation

From the convolution representation it follows that the Fourier transform of the wavelet transform (with respect to the translation parameter u) is, in view of the convolution theorem,

$$\hat{Wf}(s,\omega) = \hat{f}(\omega)\ \mathcal{F}\bar{\psi}_s^*$$

$$= \hat{f}(\omega)\,(s^{-1/2})\hat{\psi}^*(\omega/s) \qquad (8)$$

(here the symbol $\mathcal{F}$ and the "circumflex" ^ have been used to denote Fourier transformation).

Inversion of the transform

It can be proved that the wavelet transform can be inverted as

$$f(x)=$$

$$(1/C_\psi)\int_{-\infty}^{\infty}\int_{-\infty}^{\infty} Wf(s,u)\ \psi_s(x-u)\,ds\,du \qquad (9)$$

where $C_\psi=\int_{-\infty}^{\infty}\frac{|\hat{\psi}(\omega)|^2}{|\omega|}d\omega \qquad (10)$

From this expression it can be seen that the function f(x) can be thought of as a superposition of the various wavelets.

Passing bands and bandwidths

In what follows we will assume that $\psi(x)$ is normalized so

$$\int_{-\infty}^{\infty}|\psi(x)|^2\,dx = \int_{-\infty}^{\infty}|\hat{\psi}(\omega)|^2\,d\omega = 1 \qquad (11)$$

The center of the passing band of $\hat{\psi}(\omega)$ is calculated as

$$\omega_0=\int_0^{\infty}\omega\ |\hat{\psi}(\omega)|^2\,d\omega \qquad (12)$$

Remark: usually ψ is real so $|\hat{\psi}(\omega)|=|\hat{\psi}(-\omega)|$ and the integral from $-\infty$ to $+\infty$ would give zero . That's why the integrals are taken from 0 to $+\infty$.

The r.m.s. bandwidth of $\hat{\psi}(\omega)$ around ω_0 is defined, consequently, as σ_ω where

$$\sigma_\omega^2 =\int_0^{\infty}(\omega-\omega_0)^2|\hat{\psi}(\omega)|^2\,d\omega \qquad (13)$$

The center of the passing band of $\hat{\psi}(\omega/s)$ (and consequently of $\mathcal{F}\psi_s$) is, then,

$$\int_0^{\infty}\omega\ |\hat{\psi}^*(\omega/s)|^2\,d\omega\left[\int_0^{\infty}|\hat{\psi}^*(\omega/s)|^2\,d\omega\right]^{-1} =$$

$$s\int_0^{\infty}\omega\ |\hat{\psi}(\omega)|^2\,d\omega = s\omega_0 \qquad (14)$$

The rms bandwidth of $\hat{\psi}(\omega/s)$ is , since

$$\int_0^\infty (\omega-\omega_0)^2 |\hat{\psi}(\omega/s)|^2 \, d\omega \Big[\int_0^\infty |\hat{\psi}^*(\omega/s)|^2 \, d\omega \Big]^{-1} = s^2 \sigma_\omega^2 \qquad (15)$$

given by $s\,\sigma_\omega$.

Thus we see that ψ_s represents a function with frequencies around $s\omega_0$ with rms deviation $s\,\sigma_\omega$.

Space localization

Performing the same sort of calculations, but now in real space, one finds that the wavelet is centered around zero (provided one assumes that $|\psi(x)|$ is even) since

$$\int_{-\infty}^{\infty} x\, |\psi(x)|^2 \, dx = 0 \qquad (16)$$

The r.m.s. deviation of ψ with respect to 0 is given by

$$\sigma_u^2 = \int_{-\infty}^{\infty} x^2 \, |\psi(x)|^2 \, dx \qquad (17)$$

One can easily see that $\psi_s(x-u)$ is concentrated around

$$\int_{-\infty}^{\infty} x^2 \, |\psi_s(x-u)|^2 \, dx = s\int_{-\infty}^{\infty} x^2 \, |\psi(s(x-u))|^2 \, dx = u \qquad (18)$$

The r.m.s deviation of $\psi_s(x-u)$, $\sigma_{u,s}^2$ is given by σ_u/s since

$$\int_{-\infty}^{\infty} (x-u)^2 \, |\psi_s(x-u)|^2 \, dx = \sigma_u^2 / s^2 \qquad (19)$$

so

$$\sigma_{u,s} = \sigma_u / s. \qquad (20)$$

Thus we see that the functions $\psi_s(x-u)$ are centered around u with rms deviation σ_u/s.

Phase space localization

The wavelet transform is a decomposition in functions which are reasonably well localized in both space and spatial frequency (or time and frequency), of course within the limitations of the uncertainty principle $\sigma_u \sigma_\omega \geq 1/2$.

Perhaps the simplest example of time-frequency localization is a musical score in which one states when a note is to be played and what its frequency is (but notice that it is impossible to state both with infinite accuracy).

From the previous section it can be seen that phase space can be divided in cells as shown in figure 1.

Notice that the size of the cells varies with s.

Discrete transforms - sampling

In practice one works with transforms in which the variables s and u are not continuous but sampled instead.

In order to conform to the shape of the cells (see previous section), the sampling is chosen to be of the form

$$s=\alpha^j \,, \; j \in \mathbb{Z}, \; \alpha \in \mathbb{R}$$
$$u=n\beta/\alpha^j, \; n \in \mathbb{Z}, \; \beta \in \mathbb{R} \qquad (21)$$

For the case $\alpha=2$ an interesting interpretation can be given. Since s labels frequencies (the centers of the passing bands) the parameter j labels the "octaves". On the other hand the bandwidths go as 1/s so if one starts with a "mother wavelet" and one thinks of it as as musical note, say C, then the wavelet for j=1 will correspond to a half note C′ (C one octave higher), j=2 corresponds to a quarter note C′′ and so forth. For this reason a wavelet transform is like giving the "score" of the signal.

Some heuristics

Consider a microscope with point spread function (in one dimension) t(x) and transfer function $T(\omega)=\hat{t}(\omega)$.

An object $V(y)= \delta(y-y_0)$ will form an image $t(y-y_0)$ so the general image from object V(y) will be

$$\phi(x) = \int t(y-x)V(x) \, dx \qquad (22)$$

Next we consider a series of microscopes with point spread functions t(sx) where $s > 0$. The parameter s controls the resolution, the higher s the better the resolution of the instrument.

If we define $\psi(x)$ by

$$\psi(x)= t^*(-x \,) \quad \phi(x)= s^{-1/2} \, WV(s,x). \qquad (23)$$

The transfer function is, then

$$T(\omega)= \hat{\psi}^*(\omega) \qquad (24)$$

so the wavelet transformation describes (except for multiplicative factors) the image of an object V(x) with point spread function $t(x)= \psi^*(-sx)$.

Revealing edges

Consider a step s(x) defined as $s(x)=-1/2$ for $x<0$ and $s(x)=1/2$ for $x>=0$.

It has the well known property that $ds(x)/dx = \delta(x)$.

Consider

$$h(x)= \int_{-\infty}^{\infty} \psi(y) \, s(x-y) \, dy \qquad (25)$$

then taking derivatives

$$dh/dx = \int_{-\infty}^{x} \psi(y) \, \delta(x-y) \, dy = \psi(x)$$

$$\text{so } h(x)= \int_{-\infty}^{x} \psi(x) \, dx \qquad (26)$$

meaning that at the edges the wavelet transform will produce an integral of the wavelet function. Edges can be emphasized by proper choice of wavelet.

Scaling and shifting properties

For some purposes it is useful to note that if the function f is changed so $f(x) \longrightarrow f(x-b)$

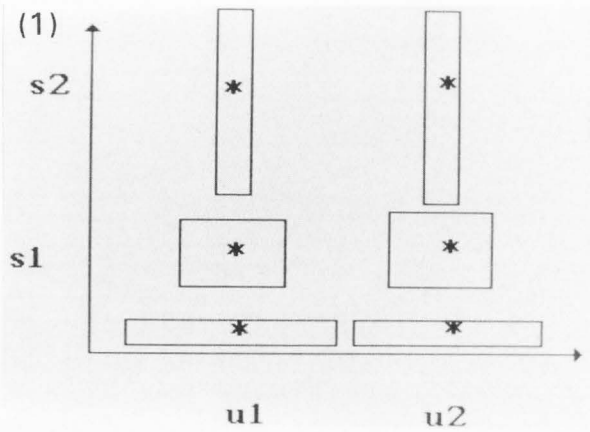

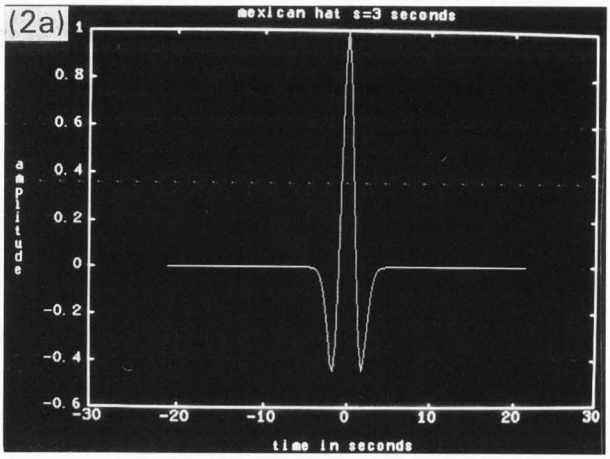

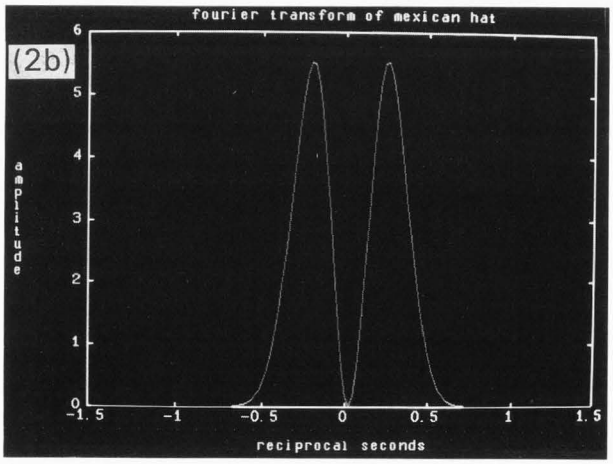

Figure 1. Illustration of the phase-space partition achieved by the discrete wavelet transform. The space is divided into unequal cells with the same area.

Figure 2. The Mexican Hat shown in real space (**a**) and in reciprocal space (**b**).

then the transforms also change and
$Wf(s,u) \longrightarrow Wf(s,u-b)$.
Similarly under a change of scale
$f(x) \longrightarrow f(\lambda x)$
the transform changes as

$$Wf(s,u) \longrightarrow \sqrt{\lambda}\ Wf(s/\lambda, u\lambda)$$

The mexican hat

One of the most popular analyzing wavelets is the so called Mexican hat given by (except for normalization constants)

$$\psi(x)=(1-x^2)\exp(-x^2/2) \qquad (27)$$

It is probably popular because of the simplicity of its form, its continuity and differentiability properties and because it is is minus one times the second derivative of the Gaussian $\exp(-x^2/2)$. It also has a smooth and fast decay at plus or minus infinity and is well localized in both real and reciprocal spaces.

This function has the appearance shown in fig. 2-a (real space)and 2-b (reciprocal space, see below).

Its Fourier transform is given by

$$\hat{\psi}(\omega)= \omega^2 \exp(-\omega^2/2). \qquad (28)$$

For small values of ω,

$$\hat{\psi}(\omega) \cong \omega^2 \qquad (29)$$

indicating that the transform for small values of ω/s behaves as a second derivative. For w in the passing band, the function and its transform are expected to be somewhat similar and for larger values of ω/s the transform will attenuate the function strongly.

Zooming

From equation(1)

$$Wf(s,u)=\int_{-\infty}^{\infty} f(x)\sqrt{s}\ \psi^*(s(x-u))\ dx$$

$$=\int_{-\infty}^{\infty} f(y/s)\sqrt{s}\ \psi^*(y-su)\ s^{-1}dy$$

$$=\int_{-\infty}^{\infty} f(y/s)\ s^{-1/2}\ \psi^*(y-su)\ dy$$

$$=s^{-1/2}[f(y/s)*\bar{\psi}_s^*(y)\ ](su) \qquad (30)$$

so one may fix $\bar{\psi}_s^*$ and rescale f. In this sense, taking the transform is like magnifying the object in a scanning electron microscope. One has a magnified image whose detail is modified by convolution with a point spread function (the shape of the beam in the SEM case).

Bidimensional case.

In 2 dimensions the transform can be defined generally as (Argoul et al. 1990):

$$Wf(A,\bar{u})=\int_{-\infty}^{\infty} f(\bar{x})\ \psi^*(\langle x-u, A(x-u)\rangle)\ d\bar{x}$$

where A is a (positive definite) linear transformation and $\langle\ \rangle$ denotes the canonical inner product in R^2. Consequently W will contain, in general, two scale factors.

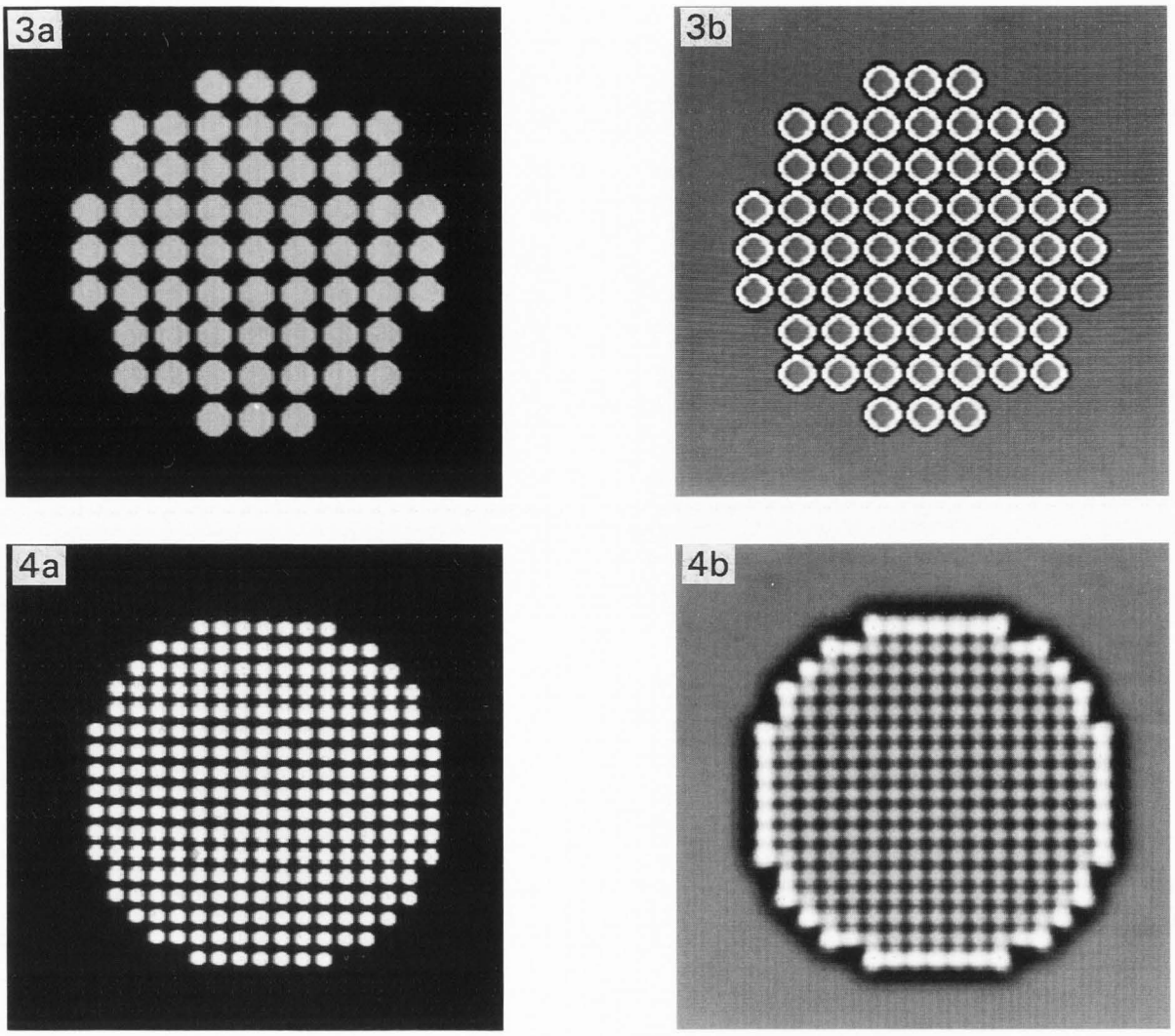

Figure 3. Example of edge enhancement by means of the wavelet transform. The image consists of an array of circles to simulate a cluster. (**a**) original image; (**b**) processed image.

Figure 4. Example of the use of wavelet transforms to obtain overall shape of an object. (**a**) original image; (**b**) processed image.

For most of our applications we have found the particular case

$$Wf(s,(u,v))=\int_{-\infty}^{\infty} f(x,y)\ s\ \psi^{*}(s(x-u),s(y-v))\ dx\ dy \qquad (31)$$

to be useful.

Results

In order to assess the use of wavelet transforms in the digital image processing of micrographs, transforms were implemented by means of the "Mexican hat" and the corresponding C language code was produced.

Synthetic objects

In figure 3-a a simulation of a cluster is shown together with its wavelet transform 3-b. Here the parameters (i.e the scaling) of the Mexican hat have been adjusted so the edges are clearly enhanced.

If the wavelet is "spread", i.e. extended in space and concentrated in frequency, it results in an enhancement of the cluster as a whole (figures 4-a and 4-b); in this case the effect of the transform is similar to a "defocus" (as can be expected from the discussion in the section on Some Heuristics) and the external shape of the cluster is enhanced at the expense of resolution. All this

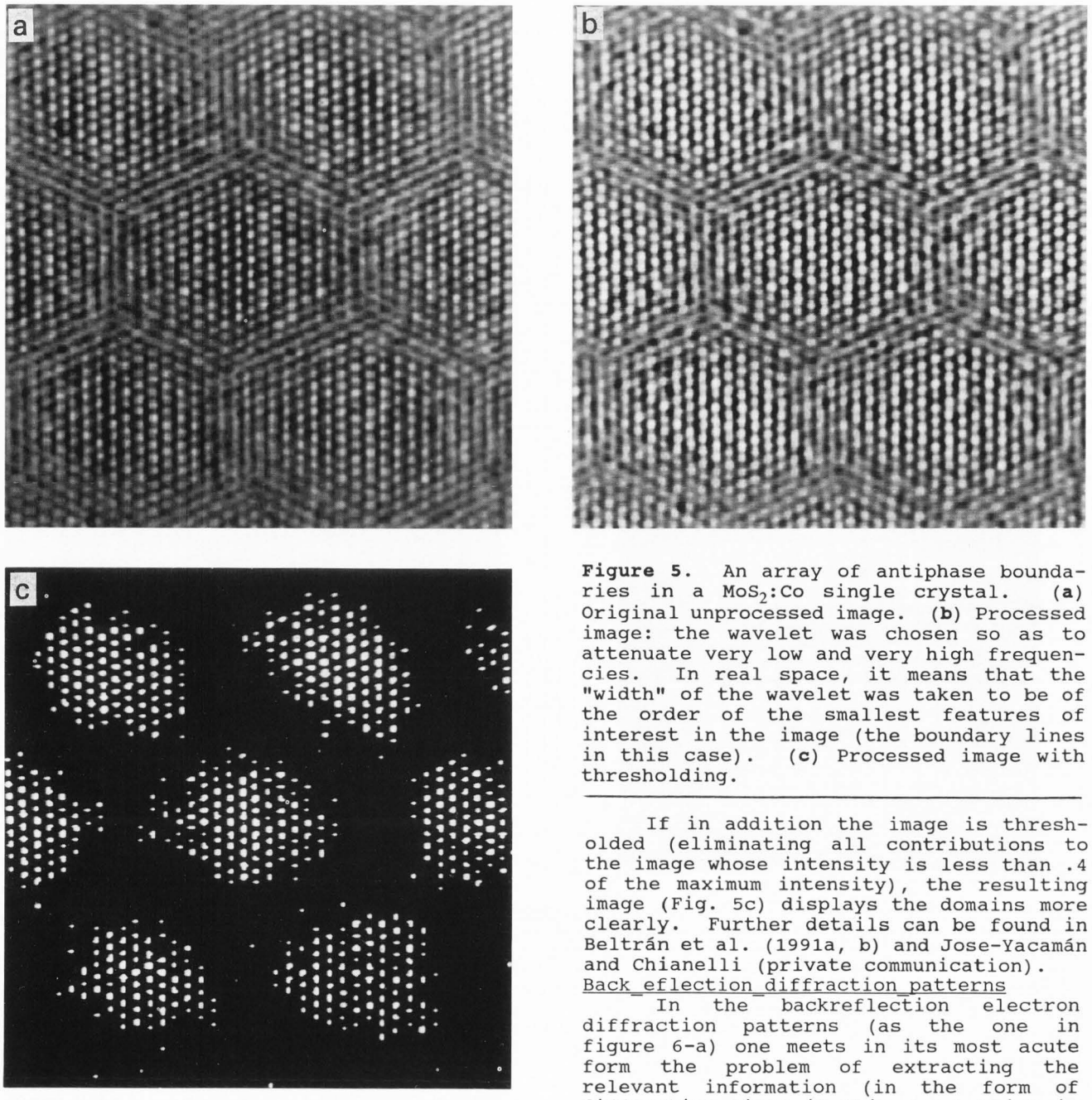

Figure 5. An array of antiphase boundaries in a MoS_2:Co single crystal. (**a**) Original unprocessed image. (**b**) Processed image: the wavelet was chosen so as to attenuate very low and very high frequencies. In real space, it means that the "width" of the wavelet was taken to be of the order of the smallest features of interest in the image (the boundary lines in this case). (**c**) Processed image with thresholding.

has been discussed in greater detail in Beltrán et al. (1991a, 1991b).

Boundaries in catalysts

In figure 5-a a high resolution image of a MoS_2:Co catalyst is shown where hexagonal domains can be clearly seen. The noise has been reduced considerably in figure 5-b (very high frequencies have been severely attenuated) whereas at the same time there has been a substantial reduction of the background (since very low frequencies have also been severely attenuated by this band-pass filter).

If in addition the image is thresholded (eliminating all contributions to the image whose intensity is less than .4 of the maximum intensity), the resulting image (Fig. 5c) displays the domains more clearly. Further details can be found in Beltrán et al. (1991a, b) and Jose-Yacamán and Chianelli (private communication).

Back eflection diffraction patterns

In the backreflection electron diffraction patterns (as the one in figure 6-a) one meets in its most acute form the problem of extracting the relevant information (in the form of diffraction lines in this case) which is immersed in a sea of noisy background.

In Figure 6-b, the same pattern is shown after a wavelet transform; the lines are now clearly visible and if the image is thresholded, the image is still clearer (in the sense of allowing an easier visual determination of the location of the lines) making it possible to measure distances and angles between lines .

In general it is observed that best results are obtained by means of the sequence transform-thresholding (in this order).

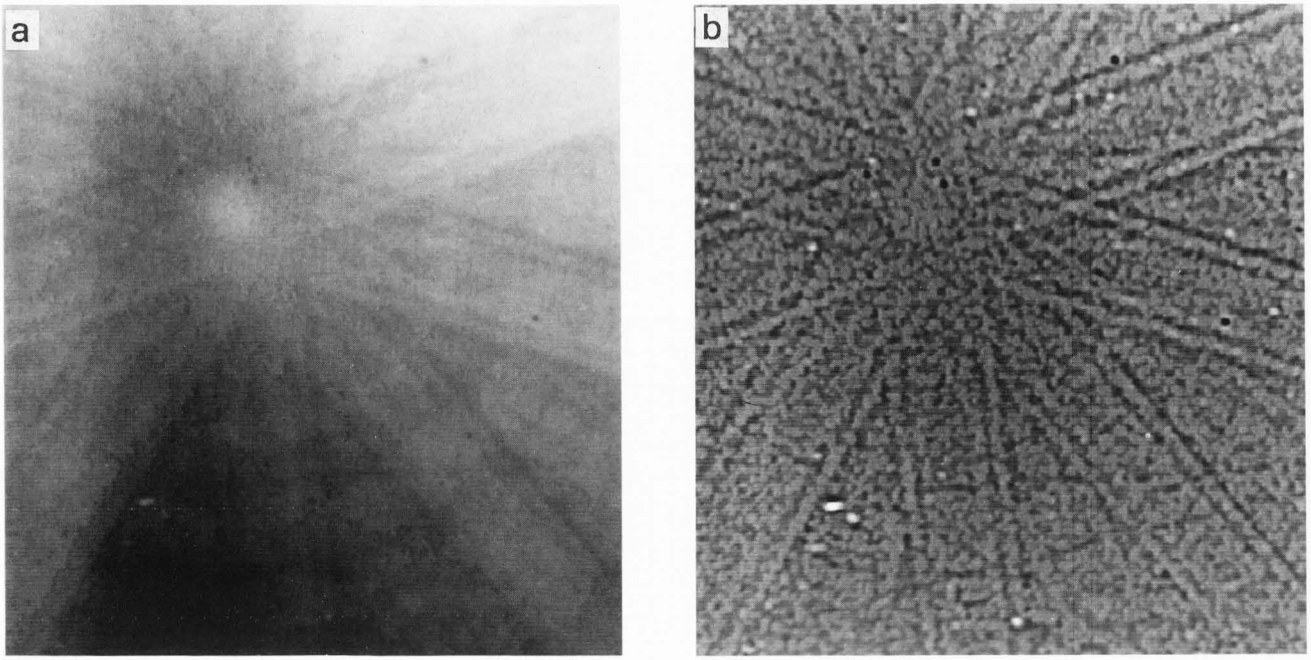

Figure 6. Electron backscattering diffraction pattern of a T-phase quasi-crystal. (**a**) Original unprocessed pattern. (**b**) Image after processing with the wavelet transform and thresholding.

The reason for the improvement in this case is that the transform was behaving basically as a second derivative (see section on the Mexican hat). The background varies slowly (low frequencies) so it is strongly attenuated and the noise components are rich in very high frequencies that are also attenuated (band-pass filter).

Small metallic particles

The transform has also been found to produce interesting results when applied to the images of small metallic particles. In Fig.7-a a multiply twinned gold particle is shown ; notice that it consists of several different crystals with well defined boundaries. In fig 7-b the same particle is shown after transforming and in fig. 7-c a threshold has been applied. As before the boundaries are enhanced by the processing.

Transforms of quasicrystals

In all the previous applications the scale of the wavelet has been kept fixed because in the images the scale of the detail of interest (or the resolution) is determined by the specific needs (i.e. to show boundaries, for instance).

However in many instances it is convenient to change the scale. This is the case for objects with details of interest at different scales, for this reason the wavelet transform is well suited to the study of fractals, turbulence and other phenomena with self-similarity or scaling symmetries.

Consequently it might be interesting to explore the use of the wavelet transform in the images from quasicrystals. As it is well known, the quasicrystals present self-similarity properties. There are certain scales (related to the golden mean) such that if one expands (inflates) the quasicrystal by them, the resulting structure has points that match those of the original unexpanded structure.

For this purpose a one -dimensional Fibonacci sequence given by

$$X_n = \alpha + \tau^{-1}\ \mathrm{Int}(n/\tau + \beta)$$

(where τ is the golden mean, α and β are real constants specifying an overall translation and the phason variable respectively) was transformed with various scales.

In figure 8 the transform is shown. The vertical axis represents the scales and the horizontal axis represents the position X_n in the Fibonacci sequence.

For very narrow wavelets the transform, as expected, follows the qusicrystal closely. When the scale is increased the transform still resembles the original image, but upon increasing the scale further a sudden point is reached where the transform has a very different appearance. This image corresponds to an inflation by $(1+\tau)$ of the original image as can be readily seen in the figure. The transform can be used

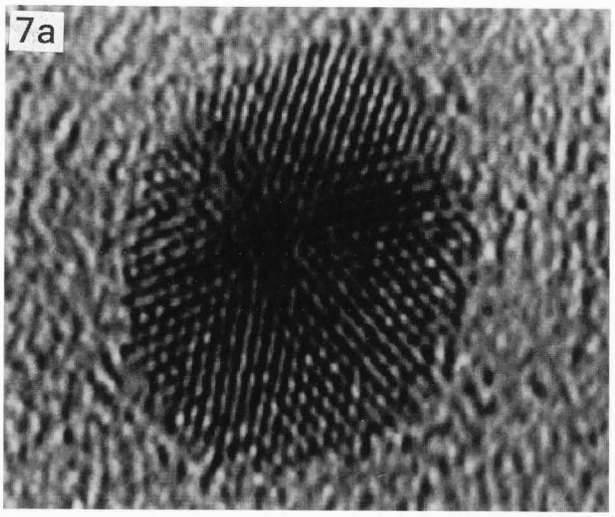

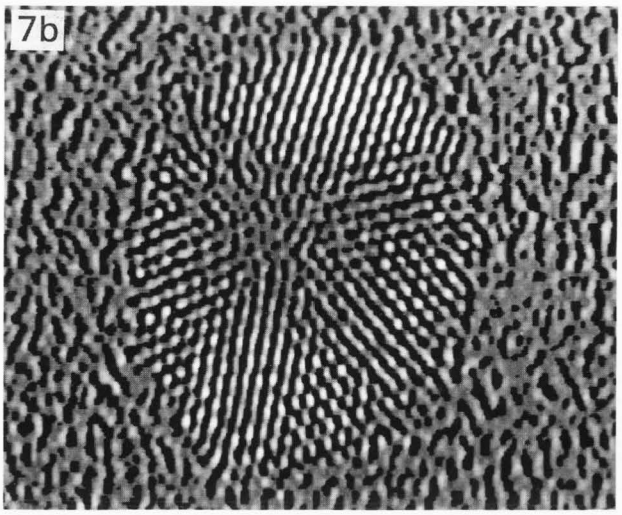

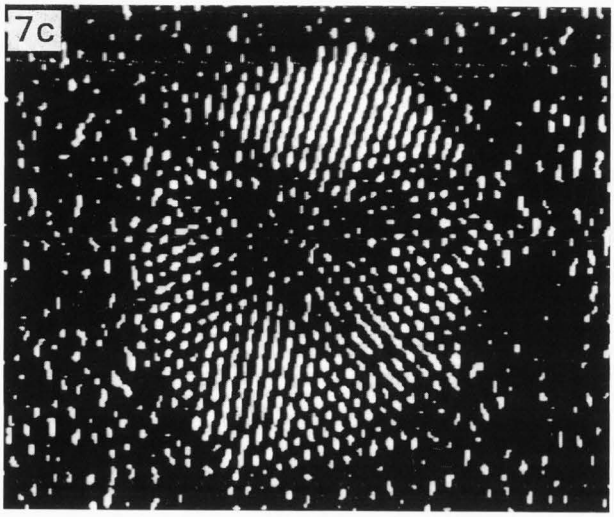

Figure 7. Multiply twinned particles of Au. (**a**) Original image; (**b**) image after wavelet transforming; (**c**) image after transforming and thresholding.

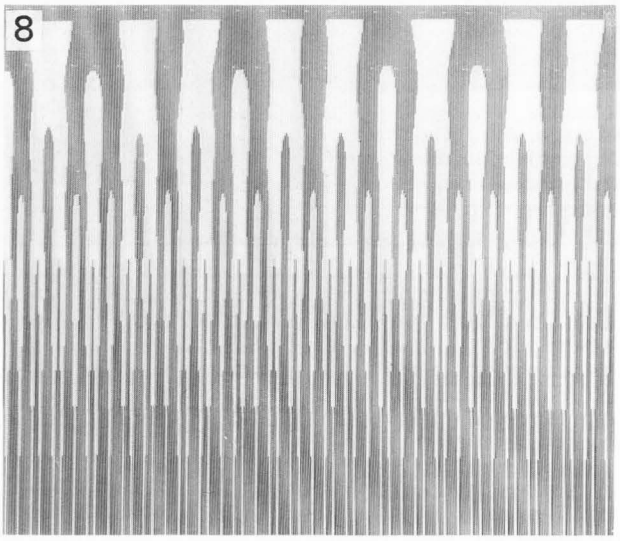

Figure 8. Wavelet transform of a one-dimensional quasi-crystal (Fibonacci sequence). The vertical axis represents the scales and the horizontal axis represents the position X_n in the Fibonacci sequence.

to study the inflations of the quasicrystal!

The reason for this behaviour is simple. As explained above, the transform returns images with a resolution given by the width of the analyzing wavelet. Since the sequence consists of an alternating array of short (S) and long (L) intervals, when the resolution reaches the scale of S the two points making S (X_n and X_n+1) can not be resolved any longer and in the image they are replaced by a single point. Thus the transformed quasicrystal is another quasicrystal in which every two positions making a short interval are replaced by a single position, simultaneously the positions corresponding to the long intervals are comparatively weak. And this is equivalent to an inflation by $1+\tau = \tau^2$. Notice that this is not the smallest inflation of the Fibonacci sequence.

Conclusions

It has been shown that many images can have specific features enhanced by means of the wavelet transforms. In particular edges and boundaries can be greatly enhanced.

For the processing of diffraction patterns the wavelet transform offers distinct advantages. Since it behaves as a band-pass filter,one can filter the

slowly varying features of the background and at the same time filter the high frequency components typical of noise. This method of background subtraction is simple and gives as good results as the ordinary methods (such as polynomial fitting of background).

A comparison of wavelet processing with standard Fourier processing has been presented in Beltrán et al. (1991-a,b).

Acknowledgements

The authors would like to thank Alfredo Sánchez for his invaluable help with the photographic work. The high resolution micrographs were taken by Luis Rendón. Some of the image handling was done with the aid of the program SAID developed, in part, by A. Granados and S. Avendaño.

The diffraction patterns were recorded at the H.H. Wills Physics Laboratory of The University of Bristol where one of the authors (D.Romeu) enjoyed the hospitality of Dr. D. Dingley.

Finally we would like to thank S. Tehuacanero for assistance in digitizing the images.

Financial support from CONACYT (grant 0534E9108)and DGAPA (grant IN104491) is acknowledged.

References

Argoul F, Arneodo A, Elezgaray J, Grasseau G. (1990). Wavelet analysis of the self-similarity of diffusion-limited aggregates and electrodeposition clusters. Phys. Rev. **A41**, 5537-5560.

Beltrán del Río L, Gómez A, Jose Yacamán M. (1991a). Image processing in TEM using the wavelet transform. Ultramicroscopy **38**, 319-324.

Beltrán del Río L, Gómez A, Jose Yacamán M. (1991b). The study of materials using wavelet image processing techniques. In: Advanced Tomographic Imaging Methods for the Analysis of Materials. MRS Proc. **217**, pp. 183-188.

Daubechies I. (1990). The wavelet transform, time-frequency localization and signal analysis. IEEE Trans. Inf. Theory **36**, 961-1005.

De Jong AF, Coene W, Van Dyck D. (1989). Image processing of HRTEM images with non-periodic features. Ultramicroscopy **27**, 53-66.

Grossmann A, Morlet J, Paul T. (1985). Transforms associated to square integrable group representations. I. General results. J. Math. Phys. **26**, 2473-2479.

Kirkland E. (1984). Improved high resolution image processing of bright field electron micrographs. I. Theory. Ultramicroscopy **15**, 151-172.

Mallat S. (1989). Multifrequency channel decompositions of images and wavelet models. IEEE Trans. Acoustics, Speech and Signal Proc. **37**, 2091-2110.

Tomita M, Hashimoto H, Ikura T, Endoh H, Yokota Y. (1985). Improvement and application of the Fourier-transformed pattern from a small area of high resolution electron microscope images. Ultramicroscopy **16**, 9-18.

Editor's Note: All of the reviewer's concerns were appropriately addressed by text changes, hence there is no Discussion with Reviewers.